JACS
JOURNAL OF THE AMERICAN CHEMICAL SOCIETY

Article

pubs.acs.org/JACS

Photoluminescence Enhancement of CdSe Quantum Dots: A Case of Organogel−Nanoparticle Symbiosis

Prashant D. Wadhavane,[†] Raquel E. Galian,[‡,⊥] M. Angeles Izquierdo,*[,†] Jordi Aguilera-Sigalat,[‡] Francisco Galindo,[†] Luciana Schmidt,[‡,§] M. Isabel Burguete,[†] Julia Pérez-Prieto,*[,‡] and Santiago V. Luis*[,†]

[†]Universitat Jaume I, Departamento de Química Inorgánica y Orgánica, Av. Sos Baynat, s/n, E-12071 Castellón, Spain

[‡]Instituto de Ciencia Molecular, Universidad de Valencia, c/Catedrático José Beltrán 2, Paterna, 46980 Valencia, Spain

[⊥]Departamento de Química Analítica, Edificio de Investigación, Universidad de Valencia, Dr. Moliner 50, 46100 Burjassot, Valencia, Spain

Supporting Information

ABSTRACT: Highly fluorescent organogels (QD−organogel), prepared by combining a pseudopeptidic macrocycle and different types of CdSe quantum dots (QDs), have been characterized using a battery of optical and microscopic techniques. The results indicate that the presence of the QDs not only does not disrupt the supramolecular organization of the internal fibrillar network of the organogel to a significant extent, but it also decreases the critical concentration of gelator needed to form stable and thermoreversible organogels. Regarding the photophysical properties of the QDs, different trends were observed depending on the presence of a ZnS inorganic shell around the CdSe core. Thus, while the core−shell QDs preserve their photophysical properties in the organogel medium, a high to moderate increase of the fluorescence intensity (up to 528%) and the average lifetime (up to 1.7), respectively, was observed for the core QDs embedded in the organogel. The results are relevant for the development of luminescent organogels based on quantum dots, which have potential applications as advanced hybrid materials in different fields.

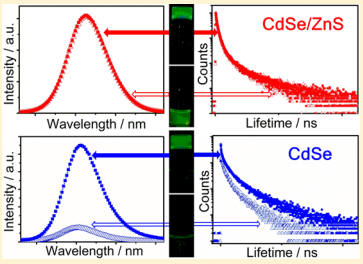

1. INTRODUCTION

The development of hybrid materials is an area of research of increasing interest due to symbiotic effects which can yield novel properties and potential applications upon combination of inorganic nanoparticles with organic scaffolds such as peptides, carbon nanotubes, polymers, or gels.[1] In particular, low molecular weight gelators are well studied functional organic molecules for the development of hybrid materials because they are known to self-assemble via noncovalent interactions to yield well ordered supramolecular structures (organogels) under favorable experimental conditions.[2] Such systems constitute a supporting environment for metallic nanoparticles of different nature, providing both stability and spatial organization to the inorganic components.[3] Thus, a broad variety of nanoparticle doped organogels based mainly on the interaction of gold[4] and silver[5] nanoparticles with self-assembled fibrillar networks have been described. Studies on the chemical structure of the gelators, and the nanoparticles have allowed a better understanding of the structural parameters determining the final properties of such systems.

Due to their intrinsic photophysical properties, emissive semiconductor nanocrystals (quantum dots, QDs) can be used in the development of fluorescent organogels, which are of great interest due to their potential applications in the preparation of optoelectronic devices and sensors.[6] It must be noted that gold nanoparticles in combination with organic fluorophores have been previously used to prepare fluorescent hybrid organogels.[4b] However, gold nanoparticles often quench the fluorescence of organic chromophores,[4a−c] and therefore, QDs appear to be very promising nanoparticles in the development of fluorescent hybrid organogels.

QDs are composed of a fluorescent core, usually CdSe or CdTe, which can be covered by an inorganic shell of a higher band gap material (ZnS, ZnSe, CdS) to yield core−shell (CS) QDs, which exhibit higher fluorescence quantum yields (Φ_F) than the core QDs in most cases.[7] Inorganic nanoparticles also need to be capped by organic ligands, which provide them with colloidal stability and determine the solubility of the nanoparticles in different media. Trioctylphosphine and trioctylphosphine oxide (T) are the most common organic ligands used in the synthesis of hydrophobic quantum dots.[8] Alternatively, amines with a long alkyl chain have also been used to stabilize different types of quantum dots.[9] Compared to organic fluorophores, QDs exhibit exceptional features, such as broad excitation bands along with narrow and size-dependent emission spectra.[10] The synthesis and characterization of these nanoparticles have been the object of many studies,[7b,8a,11] and different biological[10c,12] and analytical[12b,c,13] applications have been described for them. However, very few examples deal with the incorporation of quantum dots into supramolecular materials such as organogels. For instance, the groups of

Received: October 24, 2012
Published: December 7, 2012

   dx.doi.org/10.1021/ja310508r | J. Am. Chem. Soc. 2012, 134, 20554−20563

Stupp,[14] McPherson,[15] and Banerjee[16] incorporated CdS nanoparticles into self-assembled structures obtained from organogel and hydrogel-based systems. Li and co-workers described the preparation of hybrid organogels by mixing CdSeS nanocrystals with a dipeptide molecule in a gelling solution.[17] Bardelang and co-workers prepared CdSe/ZnS QD−peptide nanocomposites[18] using ultrasonic treatment and suggested the size reduction of the QDs by a peptidic amyloid supergelator, based on the blue shift of the photoluminescence emission.[18b] Very recently, the groups of Zhou and You reported the rational design of a hyperbranched molecule to prepare fluorescent CdSe and CdSe/ZnS based hybrid materials by sonication.[19] In addition, the potential application of QD-doped oganogels as chemical sensors of gases has been recently demonstrated.[18a,20]

Although these pioneering works set the basis for the development of QD-doped organogels, a number of fundamental aspects, such as (i) the influence of the QD composition on the QD/organogel mutual interaction and (ii) the potential synergic effects between the QDs and the organogel to improve the (photo)physical properties of the hybrid system, remain unexplored. In the present work we used the pseudopeptidic macrocyclic compound **1** (Figure 1A) as

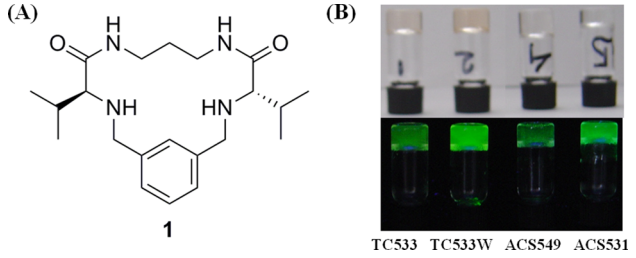

Figure 1. (A) Chemical structure of organogelator **1**. (B) Photographs of representative samples of hybrid organogels containing different types of core and core−shell QDs under room (top) and UV (bottom) light, showing the luminescence of the QDs in organogel media.

the organogelator along with different types of QDs, such as the CdSe core and the CdSe/ZnS core−shell capped with trioctylphosphine oxide and octadecylamine (ODA), as organic ligands. Our results indicate that the formation of the organogel is favored in the presence of the QDs because it is possible to reduce the concentration of gelator to form stable and thermoreversible QD−organogels. The analysis of the photophysical properties of the QDs reveals that the core−shell QDs preserve their emission intensity and fluorescence lifetime under the experimental conditions used to prepare the organogels. The fluorescence lifetimes and their corresponding contributions to the fluorescence signal follow the same pattern for each set of core−shell QDs regardless of the presence of organogelator **1**. Very importantly, the optical properties of the core QDs used in this study are in fact significantly improved in the organogel media. Thus, a high increase in the luminescence intensity, combined with a moderate increase of the average luminescence lifetime, is observed for the core QDs embedded in the organogel. Our data are in accordance with a gel-induced increase of the radiative rate constant as the main contributing factor for the fluorescence enhancement.

2. EXPERIMENTAL SECTION

2.1. Materials. All reagents were used as received without further purification. Toluene (spectroscopy grade), hexanes (spectroscopy grade), methanol (spectroscopy grade), and acetone (spectroscopy grade) were purchased from Scharlab. Cadmium oxide (CdO, >99.9%, powder), selenium (Se, 99.99%, powder, 100 mesh), trioctylphosphine oxide (T, 99%), trioctylphosphine (90%), diethylzinc solution ($ZnEt_2$), bis(trimethylsilyl) sulphide $(TMS)_2S$, 1-octadecene (ODE, 90%), oleic acid (OA, 90%), and octadecylamine (ODA, 97%) were purchased from Sigma-Aldrich. Tetradecylphosphonic acid (TDPA, 98%) was purchased from Alfa Aesar). Cyclophane **1** was synthesized according to the described experimental procedure.[21] The spectral characterization of the prepared compound **1** coincided with the reported data.

2.2. Synthesis of Quantum Dots. *2.2.1. Synthesis of Core QDs.* The CdSe QDs were synthesized following the methodology of Peng et al. with some modifications.[8a,22]

Synthesis of TC533 QDs. Briefly, the mixture of CdO (51 mg), TDPA (223 mg), and trioctylphosphine oxide (3.776 g) was heated at 300 °C under Ar until a clear solution was obtained. Then, the temperature was lowered to 270 °C and a solution of Se in trioctylphosphine (41 mg in 2.4 mL) was added and maintained during 1.5 min. The nanoparticles were precipitated in cold methanol, centrifuged three times (8000 rpm), and redissolved in toluene to yield TC533 QDs (Φ_F = 8%).

Synthesis of TC533W QDs. In order to eliminate part of the organic ligands from the TC533 inorganic surface, the nanoparticles were washed 6 times with methanol and redissolved in toluene to yield TC533W QDs (Φ_F = 3%).

Synthesis of AC527 QDs. The TC533 QDs were used to obtain CdSe QDs covered with ODA. The ligand exchange reaction was made in toluene under nitrogen atmosphere, using an amine/QD ratio of 5000:1, for 48 h. The resulting nanoparticles were precipitated, centrifuged, and washed with methanol and redissolved in toluene to yield AC527 QDs (Φ_F = 4.2%).

2.2.2. Synthesis of Core−Shell QDs. Synthesis of TCS572 QDs. In the case of CdSe/ZnS QDs capped with trioctylphosphine oxide as ligand, a one-pot Raymo et al. procedure was used.[23] In this case, the temperature of addition of Se to the trioctylphosphine solution was 220 °C and the mixture was maintained at 200 °C for 40 min. Then, the temperature was lowered to 120 °C and a solution of $ZnEt_2$ (197 mg) and $(TMS)_2S$ (250 mg) in trioctylphosphine (5 mL) was added dropwise. After addition, the mixture was maintained at 70 °C for 24 h. After cooling to ambient temperature, MeOH was added and the resulting precipitate was filtered and dissolved in hexane to yield TCS572 QDs (Φ_F = 35%).

Synthesis of ACS531 QDs. The above-mentioned methodology (one pot synthesis) with some modifications was used for the synthesis[23] but using OA and ODE instead of phosphines. Briefly, CdO (51 mg), oleic acid (339 mg), and ODE (9.8 mL) were heated in a flask to 300 °C under nitrogen atmosphere. The temperature was then lowered to 220 °C and a solution of Se (39 mg) in ODE (2.5 mL) and ODA (previously heated to 220 °C for 3 h) was added. Then, the temperature was lowered to 200 °C and maintained for 10−40 min depending on the nanoparticle size desired. Subsequently, the temperature was lowered to 120 °C, a mixture of $ZnEt_2$ and $(TMS)_2S$ dissolved in ODE was added, and the temperature was maintained at 70 °C overnight. The QDs were precipitated in acetone and dissolved in hexane or toluene to yield ACS531 QDs (Φ_F = 18%).

Synthesis of ACS549 QDs. A standard procedure was applied to the ligand exchange of CdSe/ZnS QDs covered with trioctylphosphine oxide by octadecylamine to yield ACS549 QDs (Φ_F = 41%).

2.3. Photophysical Characterization. UV−visible absorption measurements were made using a Hewlett-Packard 8453 spectrophotometer. Steady-state fluorescence spectra were recorded in a Spex Fluorog 3-11 equipped with a 450 W xenon lamp. Fluorescence spectra were recorded in the front face mode. Time-resolved fluorescence measurements were done with the technique of time correlated single photon counting (TCSPC) in an IBH-5000U.

dx.doi.org/10.1021/ja310508r | J. Am. Chem. Soc. 2012, 134, 20554−20563

Table 1. Description of Core and Core−Shell QDs Used in This Study

sample	core	shell	ligand	D (nm)	λ_{abs} (nm)	λ_{em}[a] (nm)	fwhm[b] (nm)	Φ_F
TC533	CdSe		trioctylphosphine oxide	2.63 (2.5)[c]	525	533	22	0.08[d]
TC533W	CdSe		trioctylphosphine oxide	2.63 (2.5)[c]	525	533	22	0.03[d]
AC527	CdSe		octadecylamine	2.63 (2.5)[c]	520	526	24	0.04[d]
TCS572	CdSe	ZnS	trioctylphosphine oxide	3.33 (3.5)[c]	565	572	23	0.35[e]
ACS531	CdSe	ZnS	octadecylamine	2.50 (3.2)[c]	516	531	25	0.18[d]
ACS549	CdSe	ZnS	octadecylamine	2.8 (3.8)[c]	540	549	25	0.41[d]

[a] λ_{exc} = 465 nm. [b] fwhm = full width at half-maximum. [c] Calculated based on TEM images. [d] Fluorescein in NaOH (0.1 M) was used as reference (Φ_{ref} = 0.87). [e] Rhodamine 6G in EtOH was used as reference (Φ_{ref} = 0.95).

Samples were excited with an IBH 464 nm NanoLED with a fwhm of 1.4 ns and a repetition rate of 100 kHz. Data were fitted to the appropriate exponential model after deconvolution of the instrument response function by an iterative deconvolution technique, using the IBH DAS6 fluorescence decay analysis software, where reduced χ^2 and weighted residuals serve as parameters for goodness of the fit. All the samples were measured in aerated conditions, except when otherwise stated.

2.4. ^{1}H NMR and ^{31}P NMR Spectroscopy. ^{1}H and ^{31}P NMR spectra were recorded on Bruker Avance DPX300 and 400. Standard Bruker software was used for acquisition and processing routines. The NMR samples containing organogelator **1** were prepared by heating the compound (2.5 mg) in deuterated toluene (2.5 mL) to 80 °C. The resulting homogeneous mixture (0.7 mL) was transferred into a NMR tube. The samples were allowed to cool to room temperature before the measurements. The NMR samples containing the nanoparticles were prepared by dissolving TC533 QDs (7.2×10^{-4} M) or TC533W QDs (6.8×10^{-4} M) in 0.7 mL of deuterated toluene. The NMR samples containing the QDs/organogelator **1** mixture were prepared by adding TC533 or TC533W QDs to a vial containing organogelator **1** in deuterated toluene at 80 °C (gelator: 2.67×10^{-3} M in 1.4 mL of toluene, 1/QD ratio of 3.7/1 and 3.9/1 for TC533 and TC533W, respectively). The resulting homogeneous mixture (0.7 mL) was transferred into a NMR tube. The samples were allowed to cool to room temperature before the measurements.

2.5. IR Spectroscopy. Infrared measurements were performed on a Fourier transform-infrared spectrometer NICOLET 5700 (Thermo Electron Corporation). The samples were prepared as follows: organogelator **1** (5 mg) was dissolved in toluene (1 mL) by heating to 80 °C. After complete solubilization of **1**, 0.5 mL of the solution was transferred into a vial containing 0.2 mL of TC533 (organogelator/QDs was 50/1 in molar ratio). Both samples, the 4.5 remaining milliliters of organogel **1** and the nanoparticle/**1** mixture, were cooled to room temperature. After gelation, a small amount of each sample was triturated with KBr in order to prepare the pellet for IR measurements. The TC533 QDs sample was prepared by slow evaporation of the solvent (toluene) in a mortar followed by the subsequent addition of KBr. A similar procedure was followed when using an organogelator concentration lower than that needed to obtain gelation.

2.6. Transmission Electron Microscopy. Samples for transmission electron microscopy (TEM) were prepared by dissolving macrocycle **1** (6 mg/mL) in hot toluene, followed by addition of QDs to the samples at the suitable concentration to visualize the individual nanoparticles. A drop of the solution was deposited onto a holey carbon coated 300 mesh TEM copper grid and was dried under air. The dried grid was loaded into a single-tilt sample holder. The TEM samples were examined on a JEOL 2100 TEM equipped with a high resolution Gatan CCD camera (11 Mpixels). The TEM equipment was operated at 120 kV and 62 μA.

2.7. Atomic Force Microscopy. Atomic force microscopy (AFM) images were recorded under ambient conditions using a JEOL SPM-5200 operating in the tapping mode regime. Microsilicon cantilever tips (μm-mash NSC35/ALBS) with a resonance frequency of approximately 275 kHz, a tip radius curvature smaller than 10 nm, a cone angle smaller than 30°, and a spring constant of about 15 N/m were used. Height and amplitude images were measured simultaneously. The atomic force microscope samples were prepared by dissolving macrocycle **1** in hot toluene followed by addition of QDs. The clear solutions were drop cast on freshly cleaved muscovite mica and allowed to evaporate for 20 h at room temperature.

2.8. Formation of the Nanoparticle Doped Organogels. A certain amount of cyclophane **1** was placed in open vials and dissolved in toluene at 80 °C. The transparent solutions were transferred to preheated 1 cm × 1 cm × 4 cm fluorescence cuvettes (quartz) immersed in a water bath at 80 °C. Then, the different types of QDs dissolved in toluene were added at the appropriate concentrations for the photophysical measurements (typically, absorbance <0.1 at the excitation wavelength for the fluorescence experiments). The samples were allowed to cool to room temperature in the fluorescence cuvettes in the dark for 30 min.[24] The transparent nature of the gels made recording of the pertinent spectroscopic data possible.

3. RESULTS AND DISCUSSION

3.1. Selection of Quantum Dots and Organogelator. Several factors need to be considered when selecting the components to prepare hybrid organogels with suitable optical properties: (i) the inorganic nanoparticles and the gelator need to be dispersed in a compatible solvent in order to obtain a homogeneous solution of the system, (ii) the components must be stable under the experimental conditions, and iii) the resulting QD−organogel must exhibit excellent transparency for the optical characterization. Pseudopeptidic macrocycle **1** was selected because of its ability to self-assemble in a number of solvents to yield organogels with excellent optical transparency,[25] suitable to study photochemical and photophysical processes.[24,26] In a preliminary work, compound **1** in combination with commercial CdSe/ZnS QDs emitting at 480 nm were used to prepare emissive hybrid organogels demonstrating that the important photophysical properties of the QDs, such as the position of the first exciton and the emission maxima, the emission intensity, and the fluorescence lifetimes, were preserved in the organogel medium.[20] The interest of the results and the simplicity of the methodology used to prepare the transparent QD−organogels encouraged us to study the use of different types of noncommercial core and core−shell quantum dots to investigate the potential symbiotic effects between the QDs and the organogel that could lead to an improvement of the (photo)physical properties of the hybrid system. The QDs used in this work were synthesized in our lab following reported methodologies with some modifications.[8a,22,23]

As stated above, the photophysical properties of quantum dots and their potential applications depend on their chemical composition. In this study, we selected quantum dots based on CdSe core because many synthetic protocols are available to prepare this type of semiconductor nanocrystals soluble in toluene,[27] where cyclophane **1** forms transparent and stable organogels. We focused on the preparation of core and core−

shell QDs, the latter having a ZnS inorganic shell which produces nanocrystals with improved fluorescence and higher stability.[7] In addition, two different types of capping ligands often used in the preparation of QDs were introduced in order to determine their possible effect on the photophysical properties of the QD−organogel system. Table 1 summarizes the chemical composition and main characteristics of the quantum dots used in this study. Herein, the nanocrystals are labeled with a letter to denote the organic ligand on the surface (T for trioctylphosphine oxide, A for the amine derivatives), one or two letters to indicate the absence or the presence of the ZnS inorganic shell (C for core, CS for core−shell), and a three digit number which corresponds to the position of the maximum emission wavelength for each sample. The letter W denotes that this type of QDs was washed more times than the parent QDs, as indicated in the Experimental Section. The sizes of the QDs were between 2.5 and 3.3 nm, as calculated using the maximum in absorption UV−visible spectra[10d] and checked by transmission electron microscopy (TEM). The fluorescence quantum yield of the QDs is in the range of 0.18−0.41 for the CdSe/ZnS QDs and 0.03−0.08 for the CdSe QDs (Table 1). In addition, the small full width at half-maximum (fwhm) in the fluorescence spectra indicates a narrow size distribution of the QDs. This fact together with the absence of a surface trap emission band at longer wavelength shows the good quality of the QDs.

3.2. Preparation of the Nanoparticle Doped Organogels. QD−organogels can be formed by using different methods, such as ultrasound treatment,[18,19] mixing of polar and apolar solvents in different proportions,[17] or, more recently, heating of the gelator in a suitable solvent to obtain a homogeneous solution followed by cooling.[20] As demonstrated by our research group, the heating method allows direct formation of the QD−organogel after cooling at room temperature inside the fluorescence cuvettes, which is very advantageous for their complete photophysical characterization and has been used to prepare a number of organogels derived from macrocycle **1**.[20,24−26] In this case, toluene was chosen as solvent because the QDs are readily obtained in toluene and macrocycle **1** forms very transparent and stable organogels. Thus, a certain amount of cyclophane **1** was placed in a vial with toluene and heated to the boiling temperature of the solvent to completely dissolve the gelator **1**. The transparent solutions were transferred to preheated fluorescence cuvettes, and then, different toluene solutions of QDs were mixed with the clear solutions of **1** and allowed to cool down at room temperature. Stable, very transparent, and slightly red or yellow colored organogels were obtained after 30 min. They emitted green or orange luminescence upon irradiation with UV light, as shown in Figure 1B for representative examples of green emitting organogels. It must be noted that the QD−organogels obtained by addition of the QDs after complete solubilization of **1** were found to preserve the QDs photophysical properties better than if the QD-doped organogels were obtained by directly mixing **1** with the QDs and toluene, followed by heating the solution to dissolve **1**. This is because the properties of QDs are known to be sensitive to temperature and oxygen.[28] Thus, prolonged heating of the QDs in the presence of the gelator should be avoided to obtain homogeneous luminescent samples.

The presence of the semiconductor nanocrystals did not appear to have a negative effect on the stability of the as-prepared hybrid gels. In order to confirm that the nanoparticles do not destabilize the supramolecular system, the gel-to-liquid transition temperatures of the different gels were measured by the inversion vial method. The control sample without QDs was prepared in parallel to the hybrid organogels in order to obtain comparable data. Typically, the melting temperatures were 3−12 °C higher for the hybrid organogels than for the control organogel, indicating a slightly better stability of the gel in the presence of the QDs. Preliminary studies to determine the critical concentration of gelator (*ccg*) in the presence of the QDs indicated that it is possible to form stable organogels by using a lower concentration of the gelator **1** (1.2 mg/mL; 3.2 mg/mL of gelator was needed in the absence of the QDs). Such effects are in agreement with studies for other hybrid organogels doped with different types of nanoparticles[3a,f,4a,b,29] and confirm that the presence of the luminescent semiconductor nanocrystals does not disrupt the supramolecular organization of the organogel under the experimental conditions used in this study but enhance the formation of the organogel state. The complete rheological characterization of the materials was out of the scope of this article.

3.3. Photophysical Characterization of the QDs in the Different Sets of Samples. With the view to establishing the influence of the organogel media on the optical properties of the QDs, we compared them with those of related QD samples in toluene solution under the same experimental conditions. The main absorption and emission features are provided in Table 2. Overall, our results indicate that both CdSe and CdSe/ZnS QDs can be used to prepare luminescent hybrid organogels. However, different trends were observed for the core and core−shell QDs, as will be discussed below.

Table 2. Absorption and Emission Properties of Core and Core−Shell QDs in the Different Types of Samples

sample	gelator (mg/mL)	λ_{abs} (nm)	λ_{em}[a] (nm)	fwhm (nm)	ΔF[b] (%)
TC533		525	533	22	
TC533	3.2	525	533	23	268
TC533W		525	533	23	
TC533W	3.2	525	533	23	485
AC527		518	527	24	
AC527	3.2	519	529	24	528
TCS572		565	572	22	
TCS572	3.2	565	572	22	11
ACS531		516	531	25	
ACS531	3.2	516	531	25	1
ACS549	-	540	549	25	
ACS549	3.2	541	549	25	−15

[a] λ_{exc} = 465 nm. [b] $\Delta F(\%) = (F - F_{gel})/F_{sol}$, where F_{gel} is the emission intensity of the QDs in the QD−organogel and F_{sol} is the emission intensity of the QDs in toluene.

UV−visible absorption measurements reveal that the only appreciable difference in the absorption spectra of the QD−organogels was the increased baseline as a consequence of light scattering, a typical phenomenon observed in gels (Figure S1 of the Supporting Information).[26,30] In order to better compare the shape of the absorption spectra and the position of the first exciton, the corrected and normalized absorption spectra were represented and can be seen in Figure 2 for representative samples (for all the samples see Figure S2 in the Supporting Information). The first exciton peak wavelength depended on

dx.doi.org/10.1021/ja310508r | J. Am. Chem. Soc. 2012, 134, 20554−20563

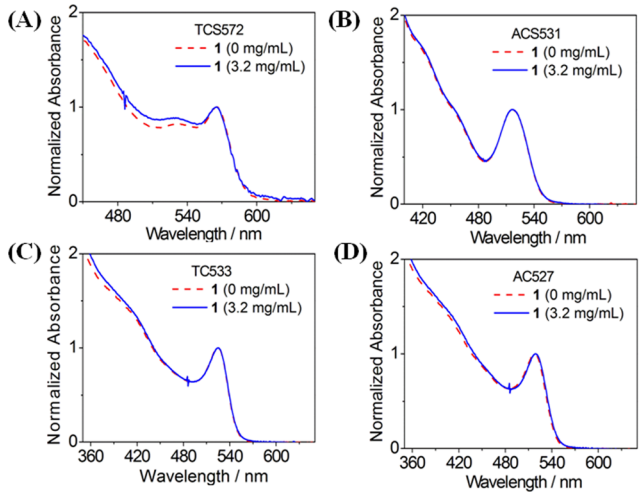

Figure 2. Corrected and normalized absorption spectra of samples prepared in toluene containing different types of QDs with and without organogelator **1**. The samples contain the following: (A) TCS572 (0.2 μM); (B) ACS531 (1.4 μM); (C) TC533 (1.8 μM); (D) AC527 (2.0 μM).

the QD diameter and did not change for most of the samples tested. Only in the case of the AC527 was a slight red shift of 1 nm observed in the organogel media.

The emission spectra are related to the quality and monodispersity of the QDs, and Figure 3 shows them for

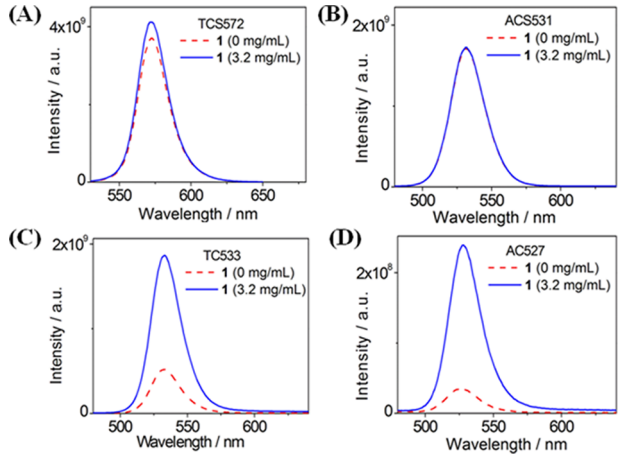

Figure 3. Emission spectra of samples prepared in toluene containing QDs with and without organogelator **1** (λ_{exc} = 465 nm). The samples contain the following: (A) TCS572 (0.2 μM); (B) ACS531 (1.4 μM); (C) TC533 (1.8 μM); (D) AC527 (2.0 μM).

representative samples of QDs in the presence and in the absence of the gelator **1** (for all the samples, see Figure S3 in the Supporting Information). The position of the emission maximum and the fwhm remained unchanged for most of the samples, regardless of the presence or absence of **1**. Only in the case of AC527 was a slight red shift of 2 nm observed in the organogel media. Consequently, the nanoparticles were very stable under the experimental conditions used to prepare the organogel and did not aggregate or oxidize, which would result in a red or blue shift, respectively, of the emission maximum, along with broadening of the emission band.

Regarding the emission intensity, two main trends were observed depending on the type of the QDs used to prepare the QD−organogels. Their different behavior was significantly marked for the presence of the ZnS inorganic shell around the CdSe core of the QDs. Thus, TCS572, ACS531, and ACS549 core−shell QDs exhibited stable emission intensity, and the gelator hardly affected that property. The low sensitivity of the core−shell QDs to organic ligands and radicals has been attributed to the efficient passivation of the CdSe surface defects by the ZnS inorganic shell,[31] which reduces significantly the effect of the gelator on the photophysical properties of the QDs.

Remarkably, in the case of the core QDs (TC533, TC533W, and AC527), a dramatic enhanced emission was observed for all of them in the hybrid organogels as compared to the QD emission in toluene under the otherwise same experimental conditions. Thus, the emission intensity of the core QDs was enhanced up to 528% in the QD−organogel system. In principle, the enhanced core-QD fluorescence in the hybrid organogels could be attributed to passivation of the QD surface defects. In fact, the relative effect of the different types of core QDs depends on the post-treatment used in the purification of the QDs. The TC533W and AC527 QDs, which required more washing steps in their preparation, as indicated in the experimental protocol, showed higher fluorescence enhancement, and this could be attributed, in part, to the presence of a higher number of defects generated in the synthetic protocol. However, as we will discuss further on in this report, this does not appear to be the main contributing factor for the impressive increase of the QD fluorescence when it is within the organogel.

It has been reported that a stabilization period may be required to obtain a stable fluorescence signal for the QDs in the presence of organic ligands.[31a] Therefore, the emission spectra of the QDs were recorded for 5 h in order to evaluate completely the effect of gelator **1** on the luminescence of the QDs (see Supporting Information Figure S4). In most cases, a stable photoluminescence signal was obtained after 1 h, which remained constant for several hours, indicating the absence of deleterious processes, which would destroy the photoluminescence of the QDs in the hybrid materials, at least for the time scale of our experiments.

The thermoreversibility of the formation and emissive properties of the gel is another important characteristic, which must be taken into account in the development of luminescent supramolecular materials. Thus, the QD−organogels were submitted to several thermal cycles by heating the cuvette up to 80 °C to obtain a clear solution and cooling to room temperature. After stabilization of the samples, the emission spectra of the QD−organogels were recorded. The cycles could be repeated in the same cuvette up to six times without any sign of fatigue or significant changes in the position, intensity, and fwhm of the emission spectra, as can be seen in Figure 4 for a representative example. These results indicate a good compatibility between the QDs and gelator **1**, in agreement with previous results obtained for other QD−organogel systems.[19,20] They are particularly interesting in the case of the core QDs because they indicate that the enhancement of the emission intensity in the presence of macrocycle **1** is preserved after several heating/cooling cycles, supporting the stabilizing role of organogelator **1** on the QD emissive properties.

Time-resolved fluorescence spectroscopy has been used to study dynamic quenching processes and to probe different heterogeneous systems.[26,32] However, to the best of our

dx.doi.org/10.1021/ja310508r | J. Am. Chem. Soc. 2012, 134, 20554−20563

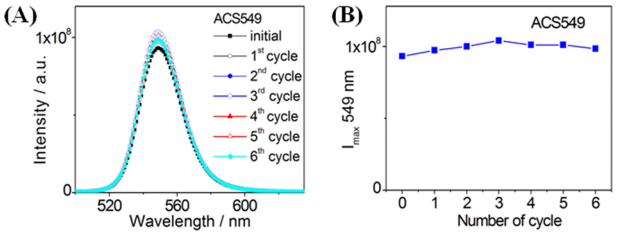

Figure 4. (A) Emission spectra of samples prepared in toluene containing QDs and organogelator **1** (λ_{exc} = 465 nm). (B) Plots of the emission intensity at the maximum emission wavelength after each cycle of melting–gelation. The samples contain organogelator **1** (3.2 mg/mL) and ACS549 (1. 0 μM).

knowledge, this technique has only been used previously by our research group to characterize commercial core–shell QDs in the organogel medium, making it possible to study the effect of the gelator concentration on the QDs lifetime.[20] Thus, in order to characterize the new hybrid supramolecular soft-materials thoroughly, time correlated single photon counting (TCSPC) studies were carried out. Fluorescent decay traces of the QDs in toluene solutions and in gelated toluene were recorded exciting at 464 nm. The emission lifetimes of the QDs are a subject of study, but the occurrence of multiphotonic processes leading to different decay processes is generally accepted.[33] Thus, the decays were fitted to a multiexponential model following eq 1, as is commonly done in the case of QDs in solution.[33] In this expression, τ_i refers to the decay times and α_i represents the amplitudes of the components.

$$I(t) = \sum_i \alpha_i \exp\left(-\frac{t}{\tau_i}\right) \quad (1)$$

The emission decay traces can be seen in Figure 5 (see all data in Supporting Information Figure S5); the emission lifetimes and their corresponding contributions to the total signal are shown in Table 3 for each set of QDs. In order to reach low χ^2 values and random distributions of the weighted residuals, the decays were fitted to a sum of three or four exponential

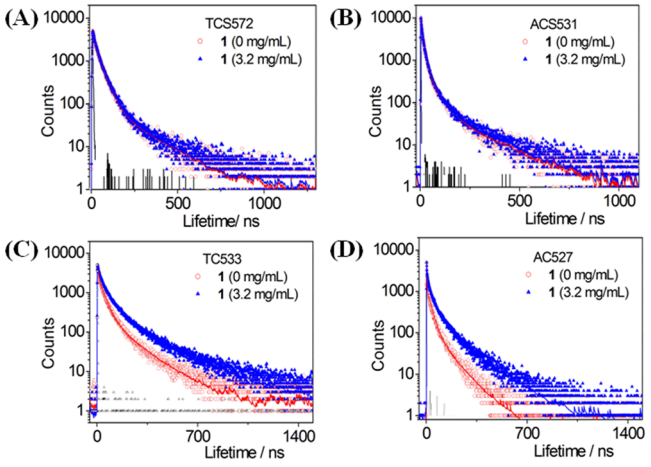

Figure 5. Fluorescence decay curves of QDs in toluene and toluene organogel containing cyclophane **1** (λ_{exc} = 464 nm, λ_{em} = 575 nm for A, λ_{em} = 530 nm for B–D). The incident light pulse is also shown (black solid line). The samples contain the following: (A) TCS572 (0.2 μM); (B) ACS531 (1.4 μM); (C) TC533 (1.8 μM); (D) AC527 (2.0 μM).

functions. The complex multiexponential decays have been attributed to a combination of surface chemistry effects and to the differences between the individual QDs present in the same nanoparticle sample.[33d,f,34] In this case, the lifetimes and pre-exponential factors differ for the sets of QDs due to the intrinsic different chemical composition of each type of QDs. However, the analysis of each type of QDs in solution and in the organogel reveals two main trends, which depend on the presence of the inorganic shell of ZnS around the CdSe core. On the one hand, the fluorescence lifetimes and their corresponding contributions to the fluorescence signal follow the same pattern for each set of core–shell QDs regardless of the presence of organogelator **1**. On the other hand, an increase in the fluorescence lifetime was observed in the case of the core QDs in the organogel medium. In order to better compare the emission lifetimes of the QDs in the presence of gelator **1**, their average lifetimes (τ_{av}) were calculated using eq 2, and the results are provided in Table 3. The average lifetime was increased by a 1.5–1.7 factor in the gels for the core QDs, while the average lifetime of the core–shell QDs was not significantly affected by the presence of the organogel structure.

$$\tau(\mathrm{av}) = \frac{\sum \alpha_i \tau_i^2}{\sum \alpha_i \tau_i} \quad (2)$$

Our results demonstrate that the dynamic properties of the core–shell QDs at the nanosecond time scale are preserved in the gel state under the experimental conditions used to prepare the organogels. The fluorescence lifetimes and their corresponding contributions to the fluorescence signal follow the same pattern for each set of core–shell QDs regardless of the presence of organogelator **1**. This could be of interest for a number of potential applications of hybrid soft supramolecular materials, such as the development of sensors based on the changes in the fluorescence lifetime of the nanoparticles as has been recently demonstrated for QDs in solution.[33e]

The emission spectra and the fluorescence lifetime of the TC533W QDs were recorded in the presence of different concentrations of the gelator to further investigate the effect of **1** on the photophysical properties of the core QDs. The relative change in the emission intensity and the average lifetime of the TC533W QDs are represented in Figures 6A and S6 as a function of the concentration of **1**. The results reveal an enhancement in the emission intensity and the fluorescence lifetime even in the presence of low concentrations of **1**, when the sample exhibits a liquid-like physical appearance. The increase of the steady-state and time-resolved values follows the same trend for low concentrations (up to 4 mM) of **1**. Remarkably, the relative average lifetime did not increase further for higher concentrations (up to 8 mM) of **1**, while the emission intensity showed an upward dependence on the concentration of **1**, indicating that the formation of the gel state had a dramatic effect on the fluorescence intensity of the QDs but not on their lifetime.

Subsequently, we estimated the radiative rate constant (k_r) and the nonradiative rate constant (k_{nr}) of the QDs in the presence of different concentrations of the macrocyle, by using eqs 3 and 4, where Φ refers to the quantum yield and τ_f refers to the lifetime (τ_{av} in this case), and we calculated the relative change in the radiative and nonradiative rate constants (Figure 6B). Data in Figure 6 reveal that the increase of the QDs fluorescence quantum yield in the presence of the gelator is mainly due to an increase in the radiative rate constant, while

dx.doi.org/10.1021/ja310508r | J. Am. Chem. Soc. 2012, 134, 20554–20563

Table 3. Fluorescence Lifetimes of Core and Core−Shell QDs in the Different Types of Samples

sample	gelator **1** (mg/mL)	$\tau_1{}^a$ (ns)	B_1 (%)	$\tau_2{}^a$ (ns)	B_2 (%)	$\tau_3{}^a$ (ns)	B_3 (%)	$\tau_4{}^a$ (ns)	B_4 (%)	τ_{av} (ns)
TC533[b]		2.7	13	19.3	61	79.3	26			56.9
TC533[b]	3.2	6.5	14	30.9	59	129.2	27			93.9
TC533W[b]		1.3	14	15.3	58	65.4	28			48.7
TC533W[b]	3.2	4.3	13	25.4	61	106.1	26			76.1
AC527[b]		1.9	24	29.5	54	115.1	22			81.2
AC527[b]	3.2	4.5	14	41.2	53	161.3	33			125.3
TCS572[c]		6.2	13	35.2	74	153.5	13			84.4
TCS572[c]	3.2	7.0	13	35.4	74	150.1	13			82.5
ACS531[b]		1.8	16	12.3	53	45.3	22	192.4	9	112.9
ACS531[b]	3.2	1.4	15	10.6	46	35.3	28	182.8	11	114.4
ACS549[b]		0.5	24	5.4	33	15.8	36	78.0	7	41.2
ACS549[b]	3.2	0.6	22	5.3	35	16.5	36	82.4	7	43.1

[a] λ_{exc} = 464 nm. [b] λ_{em} = 530 nm. [c] λ_{em} = 575 nm.

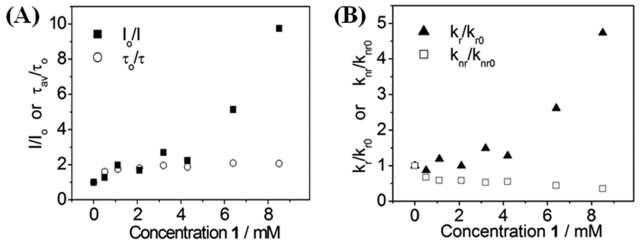

Figure 6. (A) Relative change in the emission intensities and the average lifetimes of the TC533W QDs vs concentration of **1**. (B) Relative change in the radiative rate constants and the nonradiative rate constants of the TC533W QDs vs the concentration of **1**.

the decrease of the k_{nr}, related to the reduction of surface defects that otherwise would trap excited electrons and decrease the emissive properties of the QDs, plays a minor role (Figure 6B). In the literature there are few reports that study the influence of surface ligands on the radiative rate constant of CdSe and CdSe/ZnS QDs. The mechanism for this phenomenon is not clear, but it has been suggested that the ligand induces shifts in energies of exciton states.[35] Photoluminescence excitation (PLE) spectroscopy has been used by Bawendi and co-workers[36] for mapping the electronic states of CdSe QDs. We performed preliminary PLE studies aimed to determine the effect of the gelator **1** and the gelation on the energy of the QD excited states. Figure S7 shows negligible changes between the PLE spectra. Alternatively, the boost in the k_r value of the CdSe QDs at high gelator concentration could also be due to the expected increase in the refractive index of the medium after formation of the highly entangled fibrillar network.[37] Further research is ongoing in order to clarify the effect of the macrocycle **1** on the radiative rate constants of the QDs in the gel state.

$$\Phi = \frac{k_r}{(k_r + k_{nr})} = \tau_f k_r \quad (3)$$

$$\tau_f = \frac{1}{(k_r + k_{nr})} \quad (4)$$

Organic compounds exhibiting different functional groups are known to modify the photophysical properties of QDs.[38] Pseudopeptidic macrocycle **1** contains amide and amine groups, as well as hydrophobic domains, in its chemical structure. Amide groups have been described to have no significant effects.[39] However, their role in the stabilization of the inorganic core of QDs cannot be completely ruled out, as described for the interaction of peptides exposed to semiconductor precursors.[40] On the other hand, amines can have important effects on the final properties of nanoparticles.[9a,31a,41] Therefore, the luminescent properties of the different QDs in organogel media can be understood by taking into account that gelator **1** is a multifunctional organic compound, which could also undergo ligand interdigitation with the QDs. This effect should be particularly favored by gelation, eventually influencing the QDs properties and generating organogels with improved properties and functionalities (symbiotic effect). Therefore, NMR and IR experiments were performed to get insight into the interaction of the macrocycle with the QDs.

3.4. NMR and IR Studies of the QD−Organogelator 1 System. The ^{1}H NMR spectrum of the organogelator **1** in deuterated toluene was registered in the presence of TC533 QDs, using an organogelator concentration lower than the critical concentration needed to form a stable organogel. Figure 7 shows the comparison between the representative signals of the macrocycle in the presence and the absence of the QDs, and it also shows the signals in the presence of trioctylphosphine oxide. A broadening of the signals was detected in the case of the QDs/**1** sample, which suggests the occurrence of an interaction between the organogelator **1** and

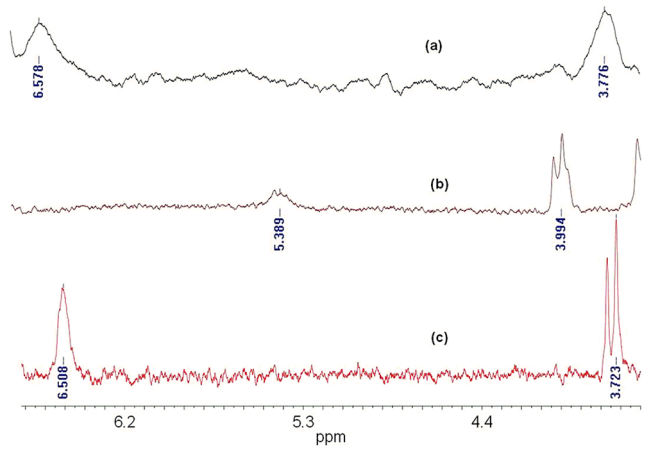

Figure 7. Bottom to top: Amplification between 3.6 ppm and 6.7 ppm of the ^{1}H NMR spectrum of the organogelator **1** (2.67×10^{-3} M, c) in deuterated toluene compared with those of **1** in the presence of trioctylphosphine oxide (**1**/phosphine oxide molar ratio of 1000/1, b) and in the presence of TC533 QDs (7.20×10^{-4} M, a).

dx.doi.org/10.1021/ja310508r | J. Am. Chem. Soc. 2012, 134, 20554−20563

the QDs even before the organogel is formed. Moreover, it should be noted that signals for the macrocycle underwent considerable displacement in the presence of TOPO; however, this was not the case in the presence of the QDs. It seems logical to suppose that the macrocycle cannot interact with the TOPO oxygen when it is attached to the QDs surface.

The interactions between **1** and the QDs before gelation were corroborated by registering the ^{31}P NMR spectra of the deuterated toluene solutions of TC533 QDs and TC533 QDs/**1** (Supporting Information Figure S8). The spectrum of the QDs/**1** mixture showed the characteristic broadening of the phosphorus signal (centered at ca. 19 ppm), remarkably shifted to high field compared to those of trioctylphosphine oxide. The presence of the organogelator **1** provoked a considerable displacement of the broad band (centered at ca. 25 ppm) to low field. Moreover, the characteristic signals of trioctylphosphine oxide were not detected in the mixture (Figure S9), demonstrating that no significant macrocycle exchange with trioctylphosphine oxide occurred once the materials had been mixed together.

Additionally, the IR spectrum of the organogelator **1** was also registered in the presence of TC533 QDs, using an organogelator concentration lower than the critical gelation concentration. Figure 8A shows the comparison between the N−H

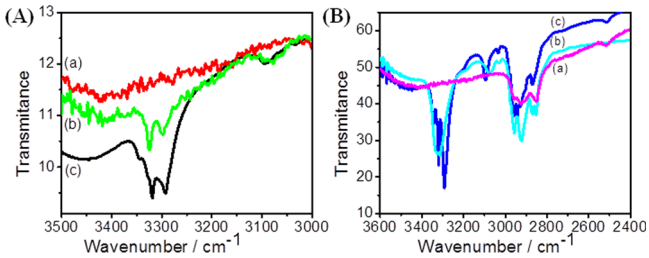

Figure 8. Comparative IR spectra of TC533 QDs (a), **1**/TC533 mixture (b, 50/1 molar ratio), and organogelator **1** (c), using KBr. (A) Compound **1** (1 mg) was dissolved in toluene (1 mL); (B) compound **1** (5 mg) was dissolved in toluene (1 mL).

bands of the macrocycle (at ca. 3300 cm^{-1}) and those in the QDs/**1** mixture, evidencing a slight increase of the N−H bond strength, indicative of a weakening of hydrogen bonding interactions. By contrast, the C−H of the aromatic bonds (at ca. 3100 cm^{-1}) shifted to lower frequencies. Similar observations were obtained for TC533W QDs. All these facts are indicative of the presence of considerable interactions between the QDs and the macrocycle **1** even before the formation of the organogel, where these interactions should be enhanced. In fact, this was corroborated by registering the IR spectrum of the hybrid organogel formed from TC533 QDs (Figures 8B and S10).

3.5. Microscopic Characterization of the QD−Organogelator 1. To get further insight into the morphological features of the hybrid systems, microscopy experiments were carried out with representative samples of xerogels containing QDs. Homogeneous toluene solutions containing different gelator concentrations were drop cast onto freshly cleaved mica and allowed to evaporate. At higher gelator concentrations, AFM images revealed the formation of a highly entangled fibrillar network distributed across the mica surface (Figure 9A, B). The samples with lower gelator concentrations made visualization of isolated fibers possible (Supporting Information Figure S11). The cross-sectional analysis revealed formation of

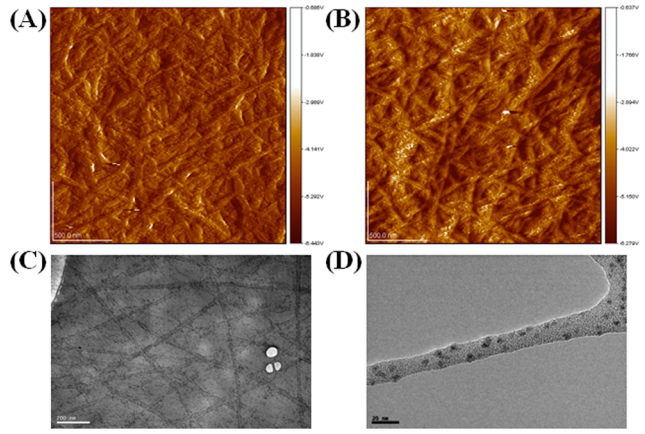

Figure 9. (A, B) AFM amplitude micrographs of xerogels prepared from solutions containing the same initial concentration of organogelator **1**. (A) Control xerogel without QDs. (B) Xerogel containing TC533 QDs. Scan area: 5.5 μm × 5.5 μm. (C, D) TEM micrographs of the fibrilar structure of cyclophane **1** xerogel containing ACS531 QDs. Scalebar: (C) 200 nm; (D) 20 nm.

long fibers with a height of around 7 nm and a width of around 111 nm for the smallest isolated fibers observed. Control experiments performed with a xerogel with the same gelator concentration but without QDs showed the formation of similar fibers with a width of 98 nm and a height of 8 nm. Overall, the AFM results indicate that the morphology of the fibrillar network formed by **1** is preserved in the presence of the QDs.

The semiconductor nanocrystals could not be visualized in the AFM micrographs because of their small size (2.2−3 nm), which was below the sensitivity of the microsilicon cantilever tips used in our experiments. Therefore, the QD-doped xerogel samples were analyzed by transmission electron microscopy (TEM). A certain volume of the different types of QDs was added to a hot solution of organogelator **1** in toluene to obtain a homogeneous sample. A drop of the transparent solution was deposited onto the holey carbon coated copper grid and dried under air overnight to prepare the corresponding xerogel. The amounts of both the organic and the inorganic components were adjusted in order to obtain a xerogel exhibiting a suitable contrast to observe both the fibrillar network and the nanoparticles. Each sample was imaged in different areas, and representative micrographs of the QD-xerogels are shown in Figure 9C, D (and Supporting Information Figures S12−S16).

Due to the holey nature of the carbon coated copper grid, the hybrid xerogel was formed both on the surface of the carbon coating and within the holes left within the amorphous material. Figure 9C shows a representative image of the xerogel formed on top of the amorphous material; the highest density of QDs is located at the edges of the fibers, suggesting that the QDs could interact preferentially with the fibers in the xerogel state. However, the fibrillar network of the gelator **1** does not always exhibit enough contrast when formed on top of the amorphous carbon material. Thus, in order to characterize the hybrid nanocomposites better, micrographs of the xerogel formed within the holes of the carbon coated copper grid were also taken (Figure 9D and Supporting Information). In all the cases, the fibrillar network of the organogel containing well dispersed QDs was obtained. The QDs exhibit the highest contrast in all TEM micrographs due to the highest electron density of the inorganic material. The individual QDs with a

dx.doi.org/10.1021/ja310508r | J. Am. Chem. Soc. 2012, 134, 20554−20563

regular shape are uniformly attached to the cross-linking gel fibers, and no QD aggregates were observed under the used experimental conditions.

TEM and AFM data show that the presence of the QDs does not disrupt the fibrillar network in the xerogel to a significant extent. These results together with those mentioned above indicate that core and core−shell QDs stabilize the fibrillar network formed by the pseudopeptidic macrocycle **1**, a role previously assigned to metallic nanoparticles on peptidic fibers. It must be taken into account that organogels have been described as supramolecular systems composed of a series of *pools of solvent* in which the mobility of the molecules is identical to the solution, but this could hardly explain the drastic changes of the emissive features of the CdSe QDs in the organogel. Indeed, the interaction of the QDs with the macrocycle starts well before the fibrillar network is formed. Therefore, the fact that the *ccg* for mixtures of QDs in organogel is lower than the *ccg* for the gelator **1** alone is a consequence of the QD acting as a nucleation site of the gelator. This could increase the local concentration of the gelator and favor the gelation. The synergistic stabilizing effect of the organogelator/QD combination is attributed to interdigitation of the gelator **1** and the QDs organic ligand, which is in good agreement with the spectroscopic results.[4b,c,18a,42] Further research is ongoing to understand the interaction of the QDs with the fibrillar network.

4. CONCLUSIONS

We have shown the symbiosis between CdSe (core and core−shell) and an organogel arising from a pseudopeptidic macrocycle in toluene. The organogel benefits from a decreased critical concentration needed to be generated in the presence of the QDs. Regarding the profits for the QDs, the most remarkable is the enhanced luminescence of the core QDs. This cooperative effect has led to highly transparent, stable, and fluorescent QD−organogels, which can be easily prepared by heating the gelator in a suitable solvent, followed by cooling at room temperature in the presence of the nanoparticles. Future studies of these materials would be addressed to investigate the use of different types of gelators to form hybrid materials doped with QDs and to study in more detail the interaction of the nanoparticles with the gelator molecules.

■ ASSOCIATED CONTENT

Supporting Information

Photophysical properties of TC533W QDs in the presence of different concentrations of gelator (Table S1), complementary spectroscopic information (Figures S1−S10), and complementary AFM and TEM micrographs of the fibrilar structure of the hybrid organogels (Figures S11−S16). This material is available free of charge via the Internet at http://pubs.acs.org.

■ AUTHOR INFORMATION

Corresponding Author

*mizquier@uji.es; julia.perez@uv.es; luiss@uji.es

Present Address

[§]Universidad Nacional de Córdoba, Departamento de Química Orgánica, Haya de la Torre y Medina Allende, s/n, 5000 Córdoba, Argentina.

Notes

The authors declare no competing financial interest.

■ ACKNOWLEDGMENTS

Financial support from the Spanish MICINN (CTQ2008-02907-E, CTQ2009-09953 and CTQ2009-14366-C02-01), GV (ACOMP/2010/258, ACOMP/2010/282 and PROMETEO/2012/020) Fundació Caixa Castelló-UJI (project P1·1B-2009-59, P1·1B2009-58) is acknowledged. P.D.W. thanks the financial support from GV (Grisolia Fellowship). We also thank MEC for the financial support (Project CTQ2011-27758), postdoctoral fellowship (L.C.S), Ramón y Cajal contract (R.E.G) and student contract (J. A-S); GVA (Project ACOMP/2009/334), and UVEG (Project UV-AE-09-5805). M. Carmen Peiro (SCIC) for technical assistance in TEM measurements and P. Clement (SCIC) for technical assistance in AFM measurements. This article is dedicated to Professor M. A. Miranda on the occasion of his 60th birthday.

■ REFERENCES

(1) (a) Descalzo, A. B.; Martinez-Mañez, R.; Sancenon, R.; Hoffmann, K.; Rurack, K. *Angew. Chem., Int. Ed.* **2006**, *45*, 5924−5948. (b) Aili, D.; Stevens, M. M. *Chem. Soc. Rev.* **2010**, *39*, 3358−3370. (c) Fabregat, V.; Izquierdo, M. A.; Burguete, M. I.; Galindo, F.; Luis, S. V. *Inorg. Chem. Acta* **2012**, *381*, 212−217. (d) Yang, Y. H.; Wen, Z. K.; Dong, Y. P.; Gao, M. Y. *Small* **2006**, *2*, 898−901. (e) Li, J.; Hong, X.; Liu, Y.; Li, D.; Wang, Y. W.; Li, J. H.; Bai, Y. B.; Li, T. J. *Adv. Mater.* **2005**, *17*, 163−166. (f) Wang, Y.-Q.; Zhang, Y.-Y.; Zhang, F.; Li, W.-Y. *J. Mater. Chem.* **2011**, *21*, 6556. (g) Sheng, W.; Kim, S.; Lee, J.; Kim, S.-W.; Jensen, K.; Bawendi, M. G. *Langmuir* **2006**, *22*, 3782−3790. (h) Yan, X. H.; Zhu, P. L.; Li, J. B. *Chem. Soc. Rev.* **2010**, *39*, 1877−1890.

(2) (a) Sangeetha, N. M.; Maitra, U. *Chem. Soc. Rev.* **2005**, *34*, 821−836. (b) George, M.; Weiss, R. G. *Acc. Chem. Res.* **2006**, *39*, 489−497. (c) Piepenbrock, M. O. M.; Lloyd, G. O.; Clarke, N.; Steed, J. W. *Chem. Rev.* **2010**, *110*, 1960−2004. (d) Hirst, A. R.; Escuder, B.; Miravet, J. F.; Smith, D. K. *Angew. Chem., Int. Ed.* **2008**, *47*, 8002−8018. (e) Dawn, A.; Shiraki, T.; Haraguchi, S.; Tamaru, S. I.; Shinkai, S. *Chem. Asian J.* **2011**, *6*, 266−282. (f) Zhu, P. L.; Yan, X. H.; Su, Y.; Yang, Y.; Li, J. B. *Chem.—Eur. J.* **2010**, *16*, 3176−3183.

(3) (a) Wu, J.; Tian, Q.; Hu, H.; Xia, Q.; Zou, Y.; Li, F.; Yi, T.; Huang, C. *Chem. Commun.* **2009**, 4100−4102. (b) Love, C. S.; Chechik, V.; Smith, D. K.; Wilson, K.; Ashworth, I.; Brennan, C. *Chem. Commun.* **2005**, 1971−1973. (c) Kar, T.; Dutta, S.; Das, P. K. *Soft Matter* **2010**, *6*, 4777−4787. (d) Ray, S.; Das, A. K.; Banerjee, A. *Chem. Commun.* **2006**, 2816−2818. (e) Amabilino, D. B.; Puigmartí-Luis, J. *Soft Matter* **2010**, *6*, 1605−1612. (f) Das, D.; Kar, T.; Das, P. K. *Soft Matter* **2012**, *8*, 2348−2365.

(4) (a) van Herrikhuyzen, J.; George, S. J.; Vos, M. R. J.; Sommerdijk, N.; Ajayaghosh, A.; Meskers, S. C. J.; Schenning, A. *Angew. Chem., Int. Ed.* **2007**, *46*, 1825−1828. (b) Sangeetha, N. M.; Bhat, S.; Raffy, G.; Belin, C.; Loppinet-Serani, A.; Aymonier, C.; Terech, P.; Maitra, U.; Desvergne, J. P.; Del Guerzo, A. *Chem. Mater.* **2009**, *21*, 3424−3432. (c) Kumar, V. R. R.; Sajini, V.; Sreeprasad, T. S.; Praveen, V. K.; Ajayaghosh, A.; Pradeep, T. *Chem. Asian J.* **2009**, *4*, 840−848. (d) Bhat, S.; Maitra, U. *Chem. Mater.* **2006**, *18*, 4224−4226. (e) Bhattacharya, S.; Srivastava, A.; Pal, A. *Angew. Chem., Int. Ed.* **2006**, *45*, 2934−2937. (f) Puigmarti-Luis, J.; Del Pino, A. P.; Laukhina, E.; Esquena, J.; Laukhin, V.; Rovira, C.; Vidal-Gancedo, J.; Kanaras, A. G.; Nichols, R. J.; Brust, M.; Amabilino, D. B. *Angew. Chem., Int. Ed.* **2008**, *47*, 1861−1865. (g) Coates, I. A.; Smith, D. K. *J. Mater. Chem.* **2010**, *20*, 6696−6702. (h) Kimura, M.; Kobayashi, S.; Kuroda, T.; Hanabusa, K.; Shirai, H. *Adv. Mater.* **2004**, *16*, 335−338.

(5) (a) Mantion, A.; Guex, A. G.; Foelske, A.; Mirolo, L.; Fromm, K. M.; Painsi, M.; Taubert, A. *Soft Matter* **2008**, *4*, 606−617. (b) Li, Y.; Liu, M. *Chem. Commun.* **2008**, 5571−5573.

(6) (a) Sagawa, T.; Fukugawa, S.; Yamada, T.; Ihara, H. *Langmuir* **2002**, *18*, 7223−7228. (b) Ajayaghosh, A.; Praveen, V. K. *Acc. Chem. Res.* **2007**, *40*, 644−656. (c) Ikeda, M.; Ochi, R.; Hamachi, I. *Lab Chip* **2010**, *10*, 3325−3334.

(7) (a) Hines, M.; Guyot-Sionnest, P. *J. Phys. Chem.* **1996**, *100*, 468−471. (b) Dabbousi, B. O.; RodriguezViejo, J.; Mikulec, F. V.; Heine, J. R.; Mattoussi, H.; Ober, R.; Jensen, K. F.; Bawendi, M. G. *J. Phys. Chem. B* **1997**, *101*, 9463−9475.
(8) (a) Peng, Z. A.; Peng, X. G. *J. Am. Chem. Soc.* **2001**, *123*, 183−184. (b) Murray, C.; Norris, D.; Bawendi, M. G. *J. Am. Chem. Soc.* **1993**, *115*, 8706−8715.
(9) (a) Talapin, D. V.; Rogach, A. L.; Kornowski, A.; Haase, M.; Weller, H. *Nano Lett.* **2001**, *1*, 207−211. (b) Yuan, C. T.; Chou, W. C.; Chen, Y. N.; Chou, J. W.; Chuu, D. S.; Lin, C. A. J.; Li, J. K.; Chang, W. H.; Shen, J. L. *J. Phys. Chem. C* **2007**, *111*, 15166−15172. (c) Shen, H.; Wang, H.; Tang, Z.; Niu, J. Z.; Lou, S.; Du, Z.; Li, L. S. *CrystEngComm* **2009**, *11*, 1733.
(10) (a) Resch-Genger, U.; Grabolle, M.; Cavaliere-Jaricot, S.; Nitschke, R.; Nann, T. *Nat. Methods* **2008**, *5*, 763−775. (b) Murray, C. B.; Kagan, C. R.; Bawendi, M. G. *Annu. Rev. Mater. Sci.* **2000**, *30*, 545−610. (c) Chan, W. C. W.; Nie, S. M. *Science* **1998**, *281*, 2016−2018. (d) Yu, W. W.; Qu, L. H.; Guo, W. Z.; Peng, X. G. *Chem. Mater.* **2003**, *15*, 2854−2860.
(11) (a) Cozzoli, P. D.; Pellegrino, T.; Manna, L. *Chem. Soc. Rev.* **2006**, *35*, 1195−1208. (b) Burda, C.; Chen, X. B.; Narayanan, R.; El-Sayed, M. A. *Chem. Rev.* **2005**, *105*, 1025−1102.
(12) (a) Bruchez, M.; Moronne, M.; Gin, P.; Weiss, S.; Alivisatos, A. P. *Science* **1998**, *281*, 2013−2016. (b) Lin, C. A. J.; Liedl, T.; Sperling, R. A.; Fernandez-Arguelles, M. T.; Costa-Fernandez, J. M.; Pereiro, R.; Sanz-Medel, A.; Chang, W. H.; Parak, W. J. *J. Mater. Chem.* **2007**, *17*, 1343−1346. (c) Smith, A. M.; Nie, S. M. *Analyst* **2004**, *129*, 672−677.
(13) (a) Zhang, F.; Ali, Z.; Amin, F.; Riedinger, A.; Parak, W. J. *Anal. Bioanal. Chem.* **2010**, *397*, 935−942. (b) Callan, J. F.; De Silva, A. P.; Mulrooney, R. C.; Mc Caughan, B. *J. Inclusion Phenom. Macrocycl. Chem.* **2007**, *58*, 257−262. (c) Martinez-Mañez, R.; Sancenon, F.; Hecht, M.; Biyikal, M.; Rurack, K. *Anal. Bioanal. Chem.* **2011**, *399*, 55−74. (d) Baù, L.; Tecilla, P.; Mancin, F. *Nanoscale* **2011**, *3*, 121−133.
(14) Sone, E. D.; Zubarev, E. R.; Stupp, S. I. *Angew. Chem., Int. Ed.* **2002**, *41*, 1705−1709.
(15) Simmons, B.; Li, S. C.; John, V. T.; McPherson, G. L.; Taylor, C.; Schwartz, D. K.; Maskos, K. *Nano Lett.* **2002**, *2*, 1037−1042.
(16) Palui, G.; Nanda, J.; Ray, S.; Banerjee, A. *Chem.—Eur. J.* **2009**, *15*, 6902−6909.
(17) Yan, X. H.; Cui, Y.; He, Q.; Wang, K. W.; Li, J. B. *Chem. Mater.* **2008**, *20*, 1522−1526.
(18) (a) Bardelang, D.; Zaman, M. B.; Moudrakovski, I. L.; Pawsey, S.; Margeson, J. C.; Wang, D. S.; Wu, X. H.; Ripmeester, J. A.; Ratcliffe, C. I.; Yu, K. *Adv. Mater.* **2008**, *20*, 4517−4520. (b) Zaman, M. B.; Bardelang, D.; Prakesch, M.; Leek, D. M.; Naubron, J. V.; Chan, G.; Wu, X.; Ripmeester, J. A.; Ratcliffe, C. I.; Yu, K. *ACS Appl. Mater Interfaces* **2012**, *4*, 1178−1181.
(19) Yan, J. J.; Wang, H.; Zhou, Q. H.; You, Y. Z. *Macromolecules* **2011**, *44*, 4306−4312.
(20) Wadhavane, P. D.; Izquierdo, M. A.; Galindo, F.; Burguete, M. I.; Luis, S. V. *Soft Matter* **2012**, *8*, 4373−4381.
(21) Becerril, J.; Bolte, M.; Burguete, M. I.; Galindo, F.; Garcia-Espana, E.; Luis, S. V.; Miravet, J. F. *J. Am. Chem. Soc.* **2003**, *125*, 6677−6686.
(22) Aguilera-Sigalat, J.; Rocton, S.; Sanchez-Royo, J. F.; Galian, R. E.; Perez-Prieto, J. *RSC Adv.* **2012**, *2*, 1632−1638.
(23) Tomasulo, M.; Yildiz, I.; Kaanumalle, S. L.; Raymo, F. M. *Langmuir* **2006**, *22*, 10284−10290.
(24) Galindo, F.; Burguete, M. I.; Gavara, R.; Luis, S. V. *J. Photochem. Photobiol., A* **2006**, *178*, 57−61.
(25) (a) Becerril, J.; Burguete, M. I.; Escuder, B.; Luis, S. V.; Miravet, J. F.; Querol, M. *Chem. Commun.* **2002**, 738−739. (b) Becerril, J.; Burguete, M. I.; Escuder, B.; Galindo, F.; Gavara, R.; Miravet, J. F.; Luis, S. V.; Peris, G. *Chem.—Eur. J.* **2004**, *10*, 3879−3890. (c) Becerril, J.; Escuder, B.; Miravet, J. F.; Gavara, R.; Luis, S. V. *Eur. J. Org. Chem.* **2005**, 481−485.
(26) Burguete, M. I.; Izquierdo, M. A.; Galindo, F.; Luis, S. V. *Chem. Phys. Lett.* **2008**, *460*, 503−506.
(27) (a) Park, J.; Joo, J.; Soon, G. K.; Jang, Y.; Hyeon, T. *Angew. Chem., Int. Ed.* **2007**, *46*, 4630−4660. (b) De Mello Donegá, C.; Liljeroth, P.; Vanmaekelbergh, D. *Small* **2005**, *1*, 1152−1162.
(28) (a) Katari, J. E. B.; Colvin, V. L.; Alivisatos, A. P. *J. Phys. Chem.* **1994**, *98*, 4109−4117. (b) Lee, W. Z.; Shu, G. W.; Wang, J. S.; Shen, J. L.; Lin, C. A.; Chang, W. H.; Ruaan, R. C.; Chou, W. C.; Lu, C. H.; Lee, Y. C. *Nanotechnology* **2005**, *16*, 1517−1521. (c) Borkovska, L. V.; Stara, T. R.; Korsunska, N. O.; Pecherśka, K. Y.; Germash, L. P.; Bondarenko, V. O. *Semicond. Phys. Quantum Electron. Optoelectron.* **2010**, *13*, 202−208.
(29) (a) Srinivasan, S.; Babu, S. S.; Praveen, V. K.; Ajayaghosh, A. *Angew. Chem., Int. Ed.* **2008**, *47*, 5746−5749. (b) Taboada, E.; Feldborg, L. N.; Pérez Del Pino, Á.; Roig, A.; Amabilino, D. B.; Puigmartí-Luis, J. *Soft Matter* **2011**, *7*, 2755−2761. (c) Das, R. K.; Bhat, S.; Banerjee, S.; Aymonier, C.; Loppinet-Serani, A.; Terech, P.; Maitra, U.; Raffy, G.; Desvergne, J. P.; Del Guerzo, A. *J. Mater. Chem.* **2011**, *21*, 2740−2750.
(30) Murata, K.; Aoki, M.; Suzuki, T.; Harada, T.; Kawabata, H.; Komori, T.; Ohseto, F.; Ueda, K.; Shinkai, S. *J. Am. Chem. Soc.* **1994**, *116*, 6664−6676.
(31) (a) Galian, R. E.; Scaiano, J. C. *Photochem. Photobiol. Sci.* **2009**, *8*, 70−74. (b) Heafey, E.; Laferriere, M.; Scaiano, J. C. *Photochem. Photobiol. Sci.* **2007**, *6*, 580−584.
(32) Burguete, M. I.; Galindo, F.; Gavara, R.; Izquierdo, M. A.; Lima, J. C.; Luis, S. V.; Parola, A. J.; Pina, F. *Langmuir* **2008**, *24*, 9795−9803.
(33) (a) Wang, X. Y.; Qu, L. H.; Zhang, J. Y.; Peng, X. G.; Xiao, M. *Nano Lett.* **2003**, *3*, 1103−1106. (b) de Mello, D.; Aacute, C.; Bode, M.; Meijerink, A. *Phys. Rev. B* **2006**, *74*, 085320. (c) Zhang, J. M.; Zhang, X. K.; Zhang, J. Y. *J. Phys. Chem. C* **2009**, *113*, 9512−9515. (d) Kloepfer, J. A.; Bradforth, S. E.; Nadeau, J. L. *J. Phys. Chem. B* **2005**, *109*, 9996−10003. (e) Ruedas-Rama, M. J.; Orte, A.; Hall, E. A. H.; Alvarez-Pez, J. M.; Talavera, E. M. *Chem. Phys. Chem.* **2011**, *12*, 919−929. (f) Jones, M.; Nedeljkovic, J.; Ellingson, R. J.; Nozik, A. J.; Rumbles, G. *J. Phys. Chem. B* **2003**, *107*, 11346−11352. (g) Rubio, J.; Izquierdo, M. A.; Burguete, M. I.; Galindo, F.; Luis, S. V. *Nanoscale* **2011**, *3*, 3613−3615.
(34) (a) Bawendi, M. G.; Carroll, P. J.; Wilson, W. L.; Brus, L. E. *J. Chem. Phys.* **1992**, *96*, 946−954. (b) Wang, X.; Qu, L.; Zhang, J.; Peng, X.; Xiao, M. *Nano Lett.* **2003**, *3*, 1103−1106. (c) Neuhauser, R. G.; Shimizu, K. T.; Woo, W. K.; Empedocles, S. A.; Bawendi, M. G. *Phys. Rev. Lett.* **2000**, *85*, 3301−3304. (d) Fisher, B. R.; Eisler, H. J.; Stott, N. E.; Bawendi, M. G. *J. Phys. Chem. B* **2004**, *108*, 143−148.
(35) Fomenko, V.; Nesbitt, D. J. *Nano Lett.* **2008**, *8*, 287−293.
(36) Norris, D. J.; Bawendi, M. G. *Phys. Rev. B* **1996**, *53*, 16338−16346.
(37) (a) Brokmann, X.; Coolen, L.; Dahan, M.; Hermier, J. P. *Phys. Rev. Lett.* **2004**, 93. (b) Vidyasagar, A.; Handore, K.; Sureshan, K. M. *Angew. Chem., Int. Ed.* **2011**, *50*, 8021−8024.
(38) Galian, R. E.; de la Guardia, M. *Trends Anal. Chem.* **2009**, *28*, 279−291.
(39) Bullen, C.; Mulvaney, P. *Langmuir* **2006**, *22*, 3007−3013.
(40) Mao, C.; Flynn, C. E.; Hayhurst, A.; Sweeney, R.; Qi, J.; Georgiou, G.; Iverson, B.; Belcher, A. M. *Proc. Natl. Acad. Sci. U.S.A.* **2003**, *100*, 6946−6951.
(41) (a) Landes, C.; Burda, C.; Braun, M.; El-Sayed, M. A. *J. Phys. Chem. B* **2001**, *105*, 2981−2986. (b) Dannhauser, T.; Oneil, M.; Johansson, K.; Whitten, D.; McLendon, G. *J. Phys. Chem.* **1986**, *90*, 6074−6076. (c) Cowderycorvan, J. R.; Whitten, D. G.; McLendon, G. L. *Chem. Phys.* **1993**, *176*, 377−386. (d) Landes, C. F.; Braun, M.; El-Sayed, M. A. *J. Phys. Chem. B* **2001**, *105*, 10554−10558. (e) Sharma, S. N.; Sharma, H.; Singh, G.; Shivaprasad, S. M. *Mater. Chem. Phys.* **2008**, *110*, 471−480. (f) Nose, K.; Fujita, H.; Omata, T.; Otsuka-Yao-Matsuo, S.; Nakamura, H.; Maeda, H. *J. Lumines.* **2007**, *126*, 21−26. (g) Liang, J. G.; Zhang, S. S.; Ai, X. P.; Ji, X. H.; He, Z. K. *Spectrochim. Acta, A: Mol. Biomol. Spectrosc.* **2005**, *61*, 2974−2978.
(42) Bose, P. P.; Drew, M. G. B.; Banerjee, A. *Org. Lett.* **2007**, *9*, 2489−2492.